JOURNAL OF MATERIALS SCIENCE 14 (1979) 184–196

The interaction between silicon nitride and several iron, nickel and molybdenum-based alloys

M. J. BENNETT, M. R. HOULTON
Materials Development Division, AERE Harwell, Didcot, Oxon, UK

Solid–solid reactions have been studied between silicon nitride and AISI 316 and 20/25/Nb austenitic stainless steels, Fecralloy* ferritic stainless steels (with and without yttrium), PE 16, Nimonic† 75, Hastelloy X‡ nickel-based alloys and a TZM molybdenum alloy. The reactant couples were heat-treated, in gettered inert gas, for up to 5161 h, at 800 to 1100° C. The temperature for the onset of measurable reaction with the iron and nickel-based alloys was between 825 and 900° C. Interaction was appreciable at 1000° C, being greatest with 20/25/Nb and least with the Fecralloy steel. The overall pattern of these reactions was similar, in that selected alloy constituents (chromium, together with iron and/or nickel where appropriate) reacted with the silicon nitride to form an adherent product, which was basically a silicide, although it also contained nitrogen. Some of the silicon and/or nitrogen released by subsequent decomposition of the primary reaction product was taken up by the alloys. In PE 16 and Hastelloy X alloys silicon was associated with molybdenum. There were several types of nitrogen pick-up: in the Hastelloy X alloy it followed a diffusion profile, while with other alloys it reacted with the constituents Ti, Al or Y to form nitrides. The surface layers on the austenitic stainless steel were denitrided, with nitrogen being transferred, via the gas phase, to a tantalum getter. With the TZM alloy no constituent was transferred to the silicon nitride. However, a silicon layer built up at the alloy surface and nitrogen was picked up, with its penetration following a diffusion profile.

1. Introduction

In some of the high temperature engineering applications for which silicon nitride is being considered, the ceramic material could be in contact with metallic alloys. A detailed knowledge is required therefore of the compatibility of silicon nitride with possible structural alloys. Previous work has been concerned primarily with metal matrix composites in which silicon nitride whiskers have been shown [1–3] to react with aluminium, iron and nickel at temperatures of interest. Recently Mehan and McKee [4] have investigated the complex reactions between the nickel-based superalloy IN-718 and silicon nitride, in air, at 1150° C.

The principal objective of the current study was to survey the chemical reactions between silicon nitride and a range of representative austenitic stainless steels (AISI 316, 20/25/Nb (20% Cr/25% Ni/Nb stabilized)) and nickel-based alloys (PE 16, Hastelloy X and Nimonic 75), together with Fecralloy ferritic stainless steels (containing 15% Cr/4% Al, with and without yttrium) and a molybdenum alloy (TZM). The observations were primarily phenomenological in nature and were aimed at evaluating such ques-

*Trade Mark of the United Kingdom Atomic Energy Authority.
†Trade Mark of Henry Wiggin and Co. Ltd.
‡Trade Mark of Union Carbide Corporation.

TABLE I Analyses of Si_3N_4 and alloys

Material	Composition (wt %)							
	Fe	Cr	Ni	Mn	Mo	Si	Nb	Zr
Fecralloy stainless steel	(79.4)	15.5				0.27		<0.01
Fecralloy (yttrium free)	(81.3)	14.3				0.16		
316 stainless steel	(64.7)	17.1	13.6	1.54	2.66	0.36		
20/25/Nb stainless steel	(53.8)	20.1	24.1	0.82		0.52	0.60	
PE 16 alloy	(33.9)	16.6	43.3	0.05	3.31	0.27		
Hastelloy X alloy	18.5	21.7	(49.5)	0.49	8.92	0.54		
Nimonic 75 alloy		19.5	(76.1)	0.4	3.34	0.16		
TZM alloy					(99.4)			0.09
Si_3N_4		0.002	0.007	0.003		57.6		
	Al	Y	Ti	Co	Ca	C	N	O
Fecralloy stainless steel	4.47	0.29		0.01		0.02	0.004	
Fecralloy (yttrium free)	4.18					0.006	0.005	
316 stainless steel						0.03	0.017	
20/25/Nb stainless steel						0.023	0.027	
PE 16 alloy	1.08		1.27	0.12		0.06	0.008	
Hastelloy X alloy	0.15			0.08		0.065	0.012	
Nimonic 75 alloy			0.4			0.13	0.029	
TZM alloy			0.5				0.0025	
Si_3N_4	0.5		0.02		0.15	1.4	38.6	1.65

tions as the temperature for onset of reaction, the severity of the attack and the nature of the reaction products.

2. Experimental

The alloy specimens were 0.5 mm thick and in the form of either 14.3 mm o.d. discs or 1 cm squares. The analyses of the alloys are given in Table I. The silicon nitride specimens (1 cm square) were cut from reaction sintered sheet (1.5 mm thick) made by the Ceramics Centre at Harwell, the analysis of which is given also in Table I. The β/α ratio of this material was 1.8 and its density was 2.2 g cm^{-3}. All specimen surfaces were lapped flat and the surface finish was equivalent to that obtained with 600 grit silicon carbide polishing paper.

For the compatibility tests, each alloy specimen was sandwiched between two silicon nitride specimens to form reaction couples, which were then stacked vertically within a closely fitting silica crucible. No additional pressure was applied to the surfaces in contact. The crucible was loaded into a silica capsule, lined with tantalum foil to act as an oxidant getter. After evacuation to a pressure less than 10^{-6} Torr, the capsule was filled with purified xenon. The capsules were heat treated at temperatures between 800 and 1100° C for periods between 1010 and 5161 h.

Small extents of reaction were determined by X-ray fluorescence, while greater attack was evaluated metallographically. The former method was based upon the supposition, substantiated experimentally, that any solid–solid reaction would involve the transference of alloy constituents to the silicon nitride surface. The iron, chromium, nickel, manganese, molybdenum, zirconium and titanium pick-ups, where appropriate, were measured. The values, expressed as μg cm^{-2} geometric surface area, were quantitative up to 20 to 40 μg cm^{-2} depending on the element. Higher uptakes represented greater attack, which could be evaluated metallographically. The composition of the reaction products and the movement of reactant constituents was examined by X-ray dispersive analysis, electron probe microanalysis and nuclear microprobe analysis. The latter technique [5] was used to determine simultaneously the nitrogen and silicon penetrations into the alloy, at a typical spatial resolution of 10 μm, by irradiation with 1.9 MeV deuterons and measurements of the characteristic protons and alpha particles emitted by the reactions $^{14}N(d, p)^{15}N$, $^{14}N(d, \alpha)^{12}C$ and $^{28}Si(d, p)^{29}Si$ respectively.

3. Results

The reactions between silicon nitride and the iron and nickel-based alloys are considered first. The results of the X-ray fluorescence procedure used to

analyse small extents of interaction were consistent with data for severe attack assessed metallographically. The X-ray fluorescence analyses of the chromium, iron and nickel pick-ups on the silicon nitride surfaces, expressed as $\mu g\,cm^{-2}$ geometric surface area, are given in Tables II and III. Although they were only quantitative up to 20 to 40 $\mu g\,cm^{-2}$, depending on the element, higher values are also quoted as they confirm the electron probe microanalyses of the principal

TABLE II The extents of reaction between silicon nitride and the Fecralloy ferritic and the 316 and 20/25/Nb austenitic stainless steels

Stainless steel	Exposure conditions		Metallic pick-up on Si_3N_4 surface ($\mu g\,cm^{-2}$)			Maximum depth of attack (μm)	
	Temperature (° C)	Time (h)	Iron	Chromium	Nickel	Si_3N_4	Steel
Fecralloy*	800	4078	0	1.5–36		NM	NM
	825	1010	0	2		NM	NM
		5009	0	8, 15		NM	NM
	900	1010	0	28		NM	NM (63)†
		5161	0	100, 155		1	2 (75)
	1000*	1173	10, 40	68, 105		2	7 (0)
		1173	110, 175	290, 395		3	4 (16)
		4030	ND	ND		20	6 (80)
	1100	1125	245–270	370–525		21	17 (375)
316	800	4824	0	0.3, 1.3	0	NM	NM
	900	1172	0	30, 38	2, 3	NM	5
	1000	1075	80	130	14	39	82
20/25/Nb	800	4078	0	0.2–0.7	0	NM	NM
	825	1010	0	1.0	0	NM	NM
		5009	0	4, 10	0	NM	NM
	900	1010	0	7.5	0	NM	NM
		5161	0	110, 150	4, 6	~2	
	1000	1173	15, 170	570, 580	430, 485	47–150	110–175

NM–none measurable; ND–not determined, gross attack.
*Results were for the yttrium bearing Fecralloy steel except that indicated at 1000° C, which was for the yttrium free material.
†Values in parentheses were depths of intergranular precipitates.

TABLE III The extents of reaction between silicon nitride and the PE 16, Hastelloy X and Nimonic 75 nickel-based alloys

Alloy	Exposure conditions		Metallic pick-up on Si_3N_4 surface ($\mu g\,cm^{-2}$)			Maximum depth of attack (μm)	
	Temperature (° C)	Time (h)	Iron	Chromium	Nickel	Si_3N_4	Alloy
PE 16	825	1010	0	1.9	0	NM	NM
		5009	0	12, 21	0.5, 1.0	NM	NM
	900	1010	0	28	0	NM	NM
		5161	0	47, 75	0–0.8	NM	1
	1000	1173	42, 65	265, 355	285, 340	6	23
Hastelloy X	800	4078	0	0.4–2.3	0	NM	NM
		4824	0	0.3, 1.3	0	NM	NM
	900	1172	0	46, 260	1.2, 14	4	3
	1000	1173	80, 125	500	585, 820	16	56
		4644	ND	ND	ND	65	65
Nimonic 75	800	4078		2.0–3.5	0	NM	NM
		4824		0.3–0.7	0	NM	NM
	900	1172		38, 70	11, 12	3	NM
	1000	1173		550	935, 1000	10	85
		4644		ND	ND	80	95

NM – none measurable; ND – not determined, gross attack.

chemical constituents of the reaction products formed on silicon nitride. Extensive reaction, for example with the 20/25/Nb stainless steel, at 1000° C, as shown in Fig. 1, resulted in the formation of silicon bearing reaction products on the silicon nitride (Figs. 1a and b). These primary reaction products contained chromium, iron (except for the Nimonic 75 alloy) and nickel (except for the Fecralloy steels) (Figs. 1c to e) from the alloy, which as a result was extensively corroded (Fig. 1f). The magnitudes of the reactions were measured metallographically as the maximum depths of the attack into the silicon nitride and of removal of material from the alloy. It should be recognized that the values given in Tables II and III are those for the cross-section through the specimen examined. Since attack was often localized to the point of contact the values quoted

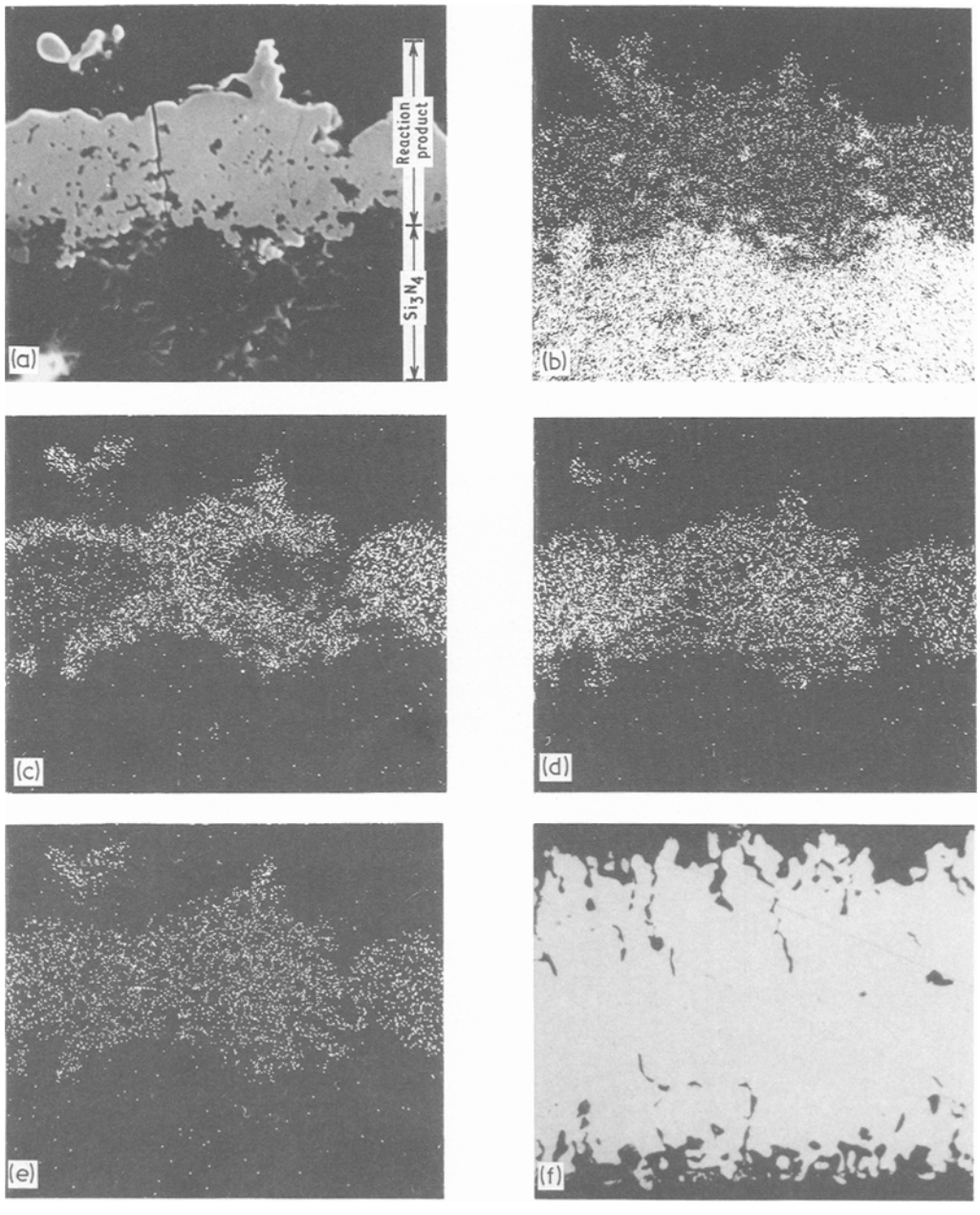

Figure 1 Micrographs of Si_3N_4 and 20/25/Nb steel after 1173 h interaction at 1000° C (a and f respectively), together with EPMA of solid reaction products produced (b–e). (a) Electron image of Si_3N_4 and reaction product (× 600); (b) Si X-ray image; (c) Fe X-ray image; (d) Cr X-ray image; (e) Ni X-ray image, and (f) 20/25/Nb stainless steel (× 97).

may not be the maximum for the specimen overall. However, these data enabled the variations of the extent of attack of each alloy with temperature and also between the alloys to be established.

The extent of interaction with each alloy increased with temperature. After 4078 to 5009 h, at 800 to 825° C, only small amounts of chromium ($<36\,\mu g\,cm^{-2}$) were transferred, probably by evaporation, onto the silicon nitride. Localized reaction was measurable metallographically at 900° C and iron and nickel, where appropriate, in addition to chromium were transported to the silicon nitride surfaces. At higher temperatures reaction was more severe and on several alloys, more uniform. At 1000° C, the order of increasing reactivity was Fecralloy steel (with or without yttrium), PE 16 alloy, Nimonic 75 alloy, Hastelloy X alloy, 316 steel and 20/25/Nb stainless steel.

Silicon and/or nitrogen diffused into the alloys concurrently with the movement of the metallic constituents from the alloy to react with the silicon nitride. The respective silicon and nitrogen distributions across the specimen cross-sections were measured by nuclear microprobe analysis and these are summarized in Table IV. The maximum and minimum levels after exposure are compared with those in the as-received material, while the depths of the affected regions and type of the distribution profile are also given. The maximum temperatures at which silicon was not observed to enter the alloys to any measurable extent were 800° C for the 316 stainless steel, 825° C for the 20/25/Nb steel and PE 16 alloy, 900° C for the Hastelloy X and Nimonic 75 alloys, and 1000° C for the yttrium-bearing Fecralloy steel. These values corresponded well to the temperatures for the onset of reaction obtained from the X-ray fluorescence analysis of the silicon nitride surfaces which contacted the alloy. At higher temperatures as a result of the solid–solid reactions, silicon diffused into the alloys and both the uptakes and depths of penetration increased with temperature, e.g. on 316 stainless steel, Fig. 2. There were two profiles for the silicon distribution through the specimen; type A, as shown in Fig. 2, in which the silicon level decreased from the surface into the bulk and type B, as for the Fecralloy steel at 1100° C shown in Fig. 3, where the level across the specimen varied within a defined scatter band. The majority of the profiles for the 316 and 20/25/Nb steels at 900

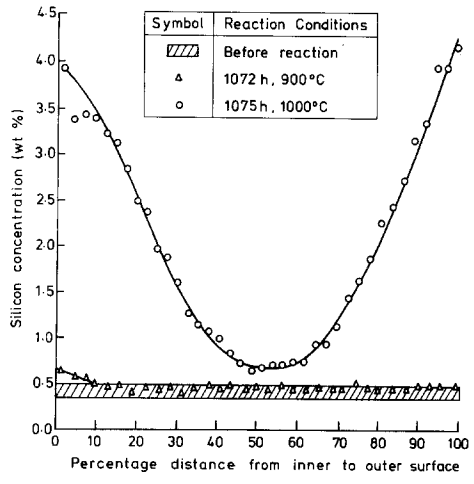

Figure 2 Silicon penetration into 316 stainless steel from reaction with silicon nitride at 900 and 1000° C.

and 1000° C, and for the PE 16, Hastelloy X (1073 h exposure only) and Nimonic 75 alloys at 1000° C were of type A. The only type B distributions were those for yttrium-free Fecralloy steel at 1000° C, the yttrium-bearing Fecralloy steel at 1100° C and the long Hastelloy X alloy exposure at 1000° C.

Any of the nitrogen produced by the silicon nitride–alloy reaction released to the gas phase would have been gettered by the tantalum. However, in the majority of cases a proportion at least reacted with the alloy. The nitrogen distribution profiles (Table IV) were more complex than those for silicon. With the austenitic stainless steels at 900° C nitrogen was picked up by the

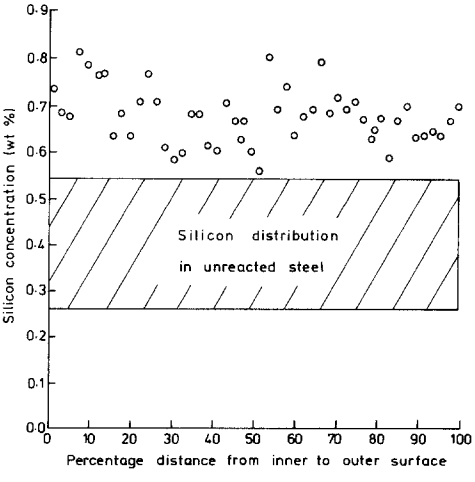

Figure 3 Silicon penetration into the Fecralloy steel from reaction with silicon nitride for 1125 h at 1100° C.

TABLE IV Silicon and nitrogen uptakes by alloys during reaction with Si_3N_4

Alloy	Exposure conditions		Silicon level (wt%)					Nitrogen level (p.p.m.)				
	Temperature (°C)	Time (h)	Initial	After exposure				Initial	After exposure			
				Max.	Min.	Depth affected (μm)	Profile type		Max.	Min.	Depth affected (μm)	Profile type
316	900	1172	0.33–0.48	0.61	0.36	60	A	160–280	520	310	500	B
	1000	1075	0.33–0.48	4.14	0.63	>250	A	160–280	1230	20	10–150	C
20/25/Nb	900	5161	0.49–0.64	0.95	0.60	95	A	190–730	390	140	500	No nitrogen uptake
	1000	1173	0.49–0.64	5.30	0.63	>250	A	190–730	2540	10	10–85	C
Fecralloy (Y-free)	1000	1173	0.16–0.24	0.43	0.23	500	B	10–13510* (single point)	4410* (single point)	10	500	No nitrogen uptake
Fecralloy	900	5161	0.26–0.53	0.53	0.35	500	No Si uptake	10–200	1310	10	40	A
	1000	1173	0.26–0.53	0.42	0.27	500	No Si uptake	10–200	830	10	100	A
	1100	1125	0.26–0.53	0.81	0.56	500	B	10–200	1580	10	500	E
PE 16	900	5161	0.26–0.64	0.74	0.23	500	No Si uptake	10–1420	3360	10	5	D
	1000	1173	0.26–0.64	2.58	0.66	>250	A	10–1420	830	10	5	D
Hastelloy X	1000	1173	0.26–0.54	7.28	1.35	>275	A	40–320	31810	230	>275	A
	1000	4644	0.26–0.54	6.40	3.34	500	B	10–120	22590	50	300	A
Nimonic 75	900	1172	0.18–0.30	0.47	0.25	500	No Si uptake	20–1850	1160	30	500	E
	1000	1173	0.18–0.30	1.59	0.33	>250	A	20–1850	2870	380	500	E
TZM	1000	4644	0.001–0.009	0.09	0.001	50	A	10–20	210	10	150	A
	1100	1125	0.001–0.009	0.96	0.001	130	A	10–20	360	10	250	A

Profile types: A–decreasing concentration from alloy surface; B–uniform concentration within defined scatter band; C–depleted region underlying surface enriched zone; D–pick-up at surface only; E–fluctuating concentration due to nitride precipitation.

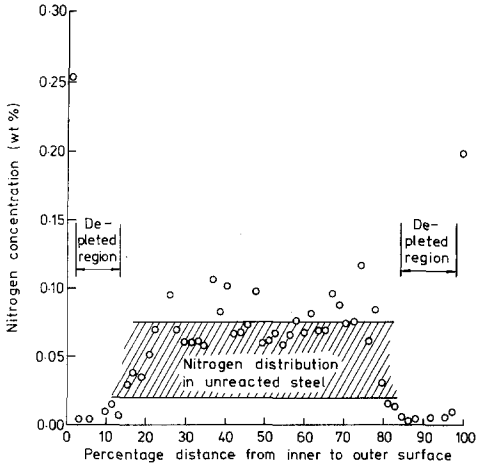

Figure 4 Nitrogen distribution across 20/25/Nb steel after reaction with silicon nitride for 1173 h at 1000° C.

316 steel with a type B profile but not by the 20/25/Nb steel. At 1000° C the nitrogen distribution across both steels was of another type C (Fig. 4), with a surface-enriched zone being followed successively by a depleted region in which the nitrogen level was less than in the original alloy and finally, a region at the specimen centre in which the nitrogen level was either comparable with or slightly greater than the initial nitrogen level. The positions of the extremities of the depleted regions are given in Table IV. There was no nitrogen uptake by the Hastelloy X alloy at 900° C, whereas at 1000° C it was substantial, with a well-defined type A diffusion profile. In the PE 16 alloy the nitrogen pick-up occurred at the surface only (type D profile) and was associated with titanium and/or aluminium (Fig. 5). There was considerable fluctuation in the nitrogen levels through the Nimonic 75 alloy at 900 and 1000° C (type E profile, Fig. 6a), which was due to the precipitation of titanium nitride (Figs. 6b and c). For the Fecralloy steel nitrogen profiles of type A were observed after reaction at 900 and 1000° C, whereas a type E profile was obtained at 1100° C. Metallographic examination of the Fecralloy steel established more clearly than the nitrogen profiles that precipitates were formed primarily in the grain boundaries (Figs. 6d and e) to a depth which was comparable at 900 to 1000° C but considerably greater at 1100° C (Table II). The precipitates were identified by EPMA as being YN (Figs. 6e and 7). Further confirmation was provided by the absence of any nitrogen pick-up and also of precipitates, in the yttrium-free Fecralloy steel at 1000° C (Table IV).

Various data were obtained on the compositions of the reaction products from the individual reactions. EPMA confirmed X-ray fluorescence

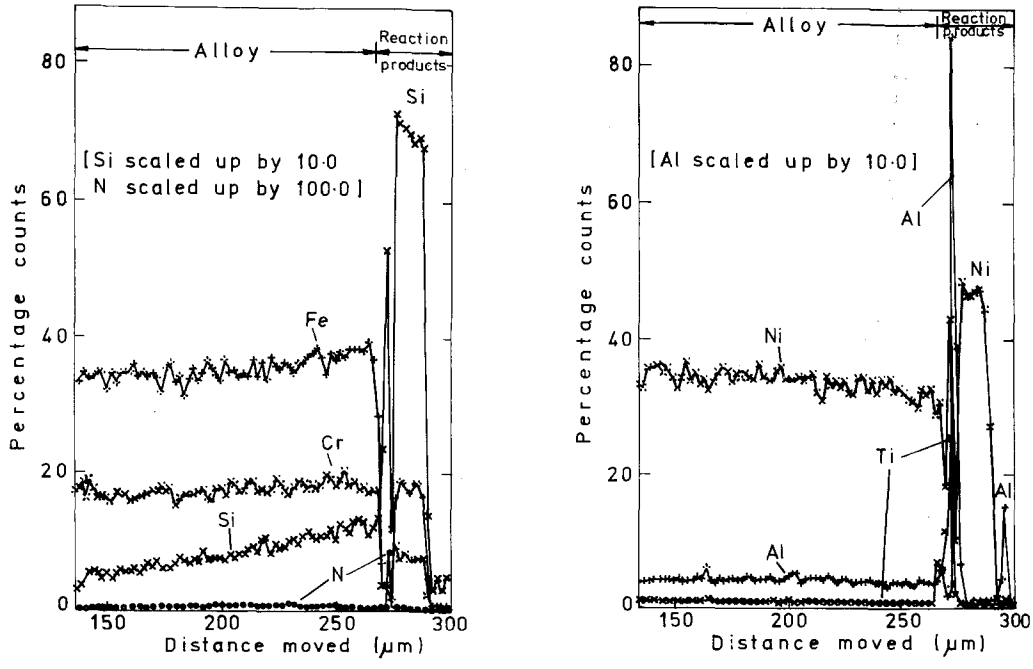

Figure 5 EPMA of reaction products formed at the PE 16 alloy surface from 1173 h interaction with Si_3N_4 at 1000° C. (The elemental traces were for the same traverse across the alloy and reaction products).

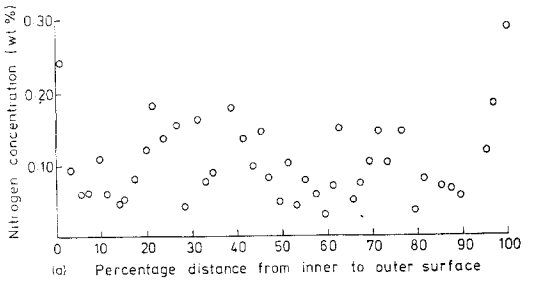

Figure 6 (a) Nitrogen profile across Nimonic 75 alloy after 1173 h reaction with Si_3N_4 at 1000° C. (b) Ti X-ray image of precipitate formed in Nimonic 75 alloy (× 4500). (c) Nitrogen X-ray image of same area as (b). (d) Electron image of grain boundaries in Fecralloy steel after 1125 h reaction with Si_3N_4 at 1100° C (× 1500). (e) Y X-ray image of same area as (d).

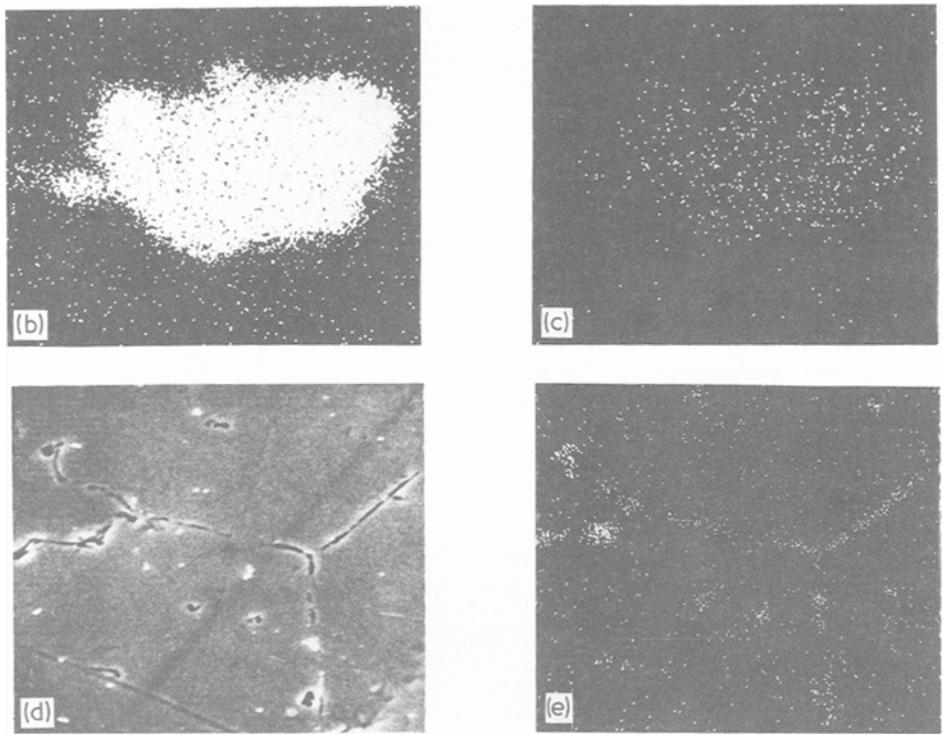

analysis that those products adhering to the silicon nitride specimens contained chromium, together with iron and/or nickel, where appropriate. The only exception was the product from reaction with the Fecralloy steel, which also contained aluminium (Figs. 8a and b), enriched particularly at the Si_3N_4–product interface. The distribution of the main metallic constituents varied (Figs. 1 and 8) but no consistent patterns could be deduced. The silicon and nitrogen profiles through a representative product of reaction with the Hastelloy X alloy at 1000° C and detectable by the presence of Fe, Cr and Ni X-rays, is shown in Fig. 9. The concentrations of these elements (average 25 and 7% respectively) were lower than in unreacted silicon nitride. The sudden reduction in nitrogen and silicon levels at about 200 μm depth from the surface was due to a fissure in the material. At depths greater than 100 μm the scatter was probably attributable to surface roughness: the statistical errors were approximately 4% Si and 0.4% N for counting statistics alone (1 σ).

The reacting metallic species diffused from 316, 20/25/Nb, Nimonic 75 and Hastelloy X alloys primarily via the grain boundaries leaving an eroded surface, e.g. see Fig. 1f for the 20/25/Nb stainless steel. This precluded a meaningful evaluation of the variation of the iron, chromium and nickel concentrations from the bulk to the edge of the alloys, e.g. as shown in Fig. 10 for the Hastelloy X alloy.

On separation of the compatibility couples no reaction products adhered to either the 316 or 20/25/Nb stainless steels, but they did so on the Fecralloy steel and the PE 16, Hastelloy X

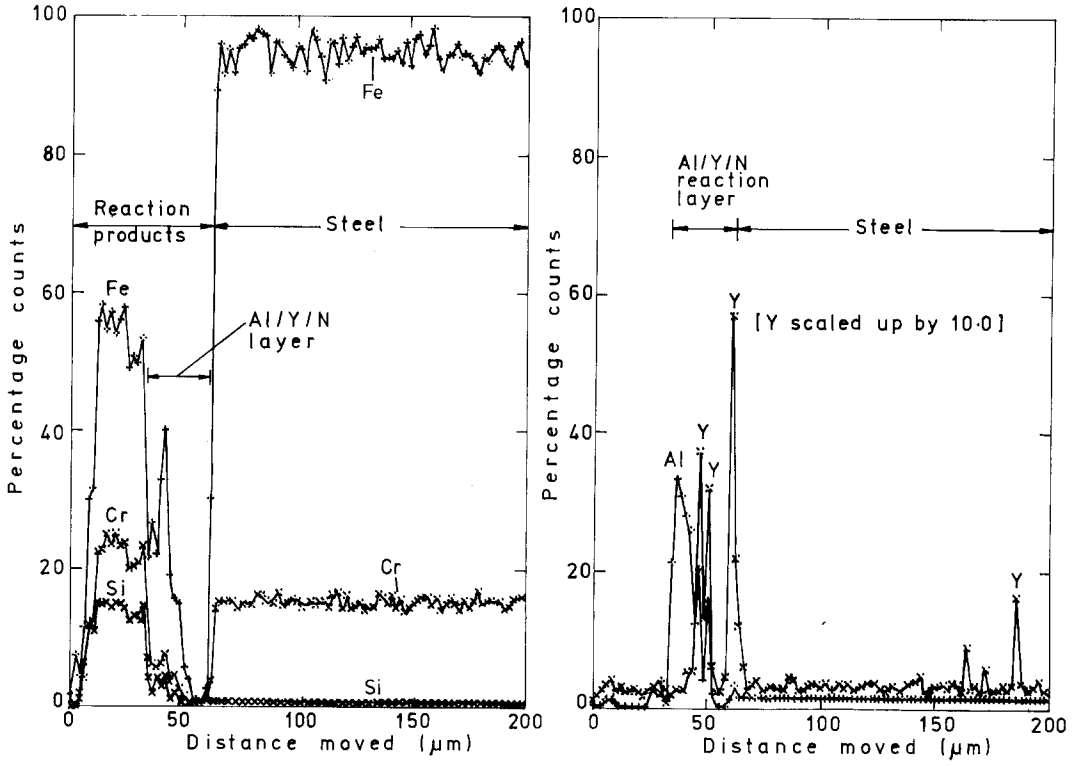

Figure 7 EPMA of Fecralloy steel after 1125 h reaction with Si_3N_4 at 1100° C. (The elemental traces were for the same traverse across the alloy and reaction products).

and Nimonic 75 alloys. Although the bulk compositions of these products were similar to those adhering to silicon nitride, in that they were a mixed chromium, iron, nickel silicide (Figs. 5, 7 and 10) there was an interfacial surface layer enriched in other alloy constituents depending on the alloy composition. Aluminium was enriched at the surfaces of the Fecralloy steel (Fig. 7), the PE 16 alloy (Fig. 5) and the Hastelloy X alloy (Fig. 10), as was yttrium at the Fecralloy steel surface (Fig. 7), while titanium concentrated at the Nimonic 75 and PE 16 alloy surfaces (Fig. 5). All three elements were associated with nitrogen, due to nitride formation. Molybdenum was associated with silicon in a surface layer on the Hastelloy X alloy (Fig. 10) and to a considerably smaller extent on the PE 16 alloy, reflecting the difference in the respective bulk molybdenum concentrations. There was also considerable silicon penetration into the Hastelloy X alloy via grain boundaries, similarly associated with molybdenum (Fig. 10).

After 4644 h at 1000° C or 1125 h at 1100° C neither molybdenum, titanium nor zirconium were transferred, within the limits of detection ($<1\,\mu g\,cm^{-2}$), from the TZM alloy to the silicon nitride. During these exposures both silicon and nitrogen diffused into the TZM alloy, although silicon was concentrated primarily at the surface (Table IV, Figs. 11 and 12). The extents of the uptakes and the depths of penetration increased with temperature, with the most significant change being the order of magnitude increase in the silicon uptake at the higher temperature.

4. Discussion

The overall patterns of the reactions between silicon nitride and both the iron- and nickel-based alloys were similar. Transport of chromium to the silicon nitride was first measured with all alloys at 800° C but could have been by evaporation rather than reaction. Solid–solid interaction occurred at 900° C and its extent increased with temperature. The principal reaction product was basically a chromium, iron and/or nickel (depending on the alloy composition) silicide, although it also contained nitrogen. The primary reaction was therefore:

$$Cr(Fe/Ni) + Si_3N_4 \rightarrow Cr(Fe/Ni)(Si, N)$$

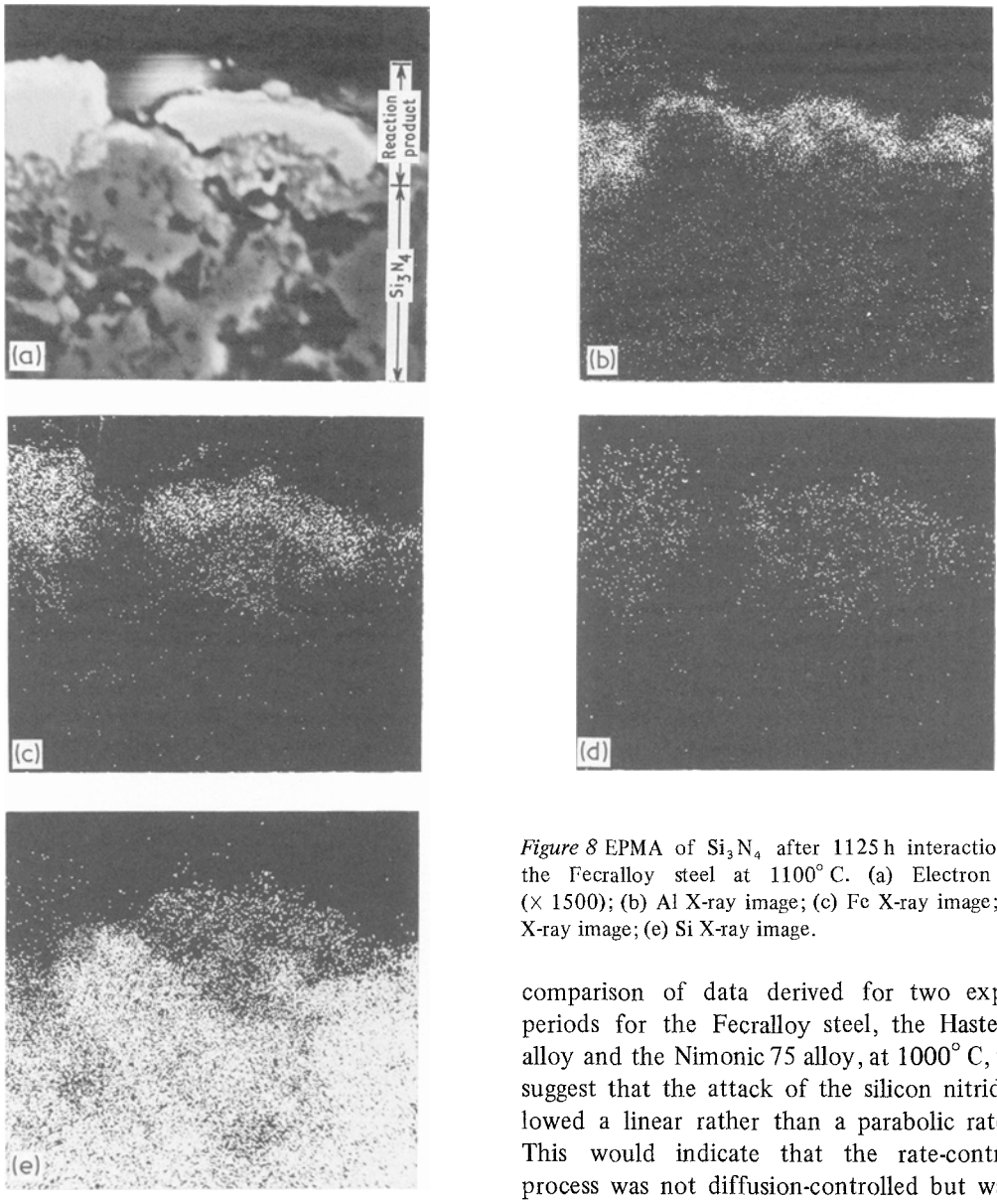

Figure 8 EPMA of Si_3N_4 after 1125 h interaction with the Fecralloy steel at 1100° C. (a) Electron image (× 1500); (b) Al X-ray image; (c) Fe X-ray image; (d) Cr X-ray image; (e) Si X-ray image.

The reaction product composition varied with temperature. Chromium was the predominant metallic species at 900° C, while iron and/or nickel became involved to a comparable extent at higher temperatures. On this basis it was not surprising that the reactivity of the alloys tended to increase with their chromium content.

Since the reaction product grew into the silicon nitride the site of the primary reaction between the alloy constituents and silicon nitride was probably the silicon nitride–reaction product interface. Unfortunately it was not possible to examine the reaction kinetics in detail but comparison of data derived for two exposure periods for the Fecralloy steel, the Hastelloy X alloy and the Nimonic 75 alloy, at 1000° C, would suggest that the attack of the silicon nitride followed a linear rather than a parabolic rate law. This would indicate that the rate-controlling process was not diffusion-controlled but was the primary reaction itself.

The other main feature of the alloy–Si_3N_4 interactions was the uptakes of nitrogen and/or silicon by the alloys. These elements probably derived from secondary reactions involving the thermal decomposition of the silicide–nitride, in which alloy constituents could have participated.

There were several well-characterized nitrogen profiles in the alloys following reaction with silicon nitride. The surface layers in the austenitic stainless steels were denitrided, probably by the decomposition of the chromium nitride present in the steel originally, with transference of the nitrogen to the tantalum getter. Nitrogen was picked up by the other alloys. In the Hastelloy X

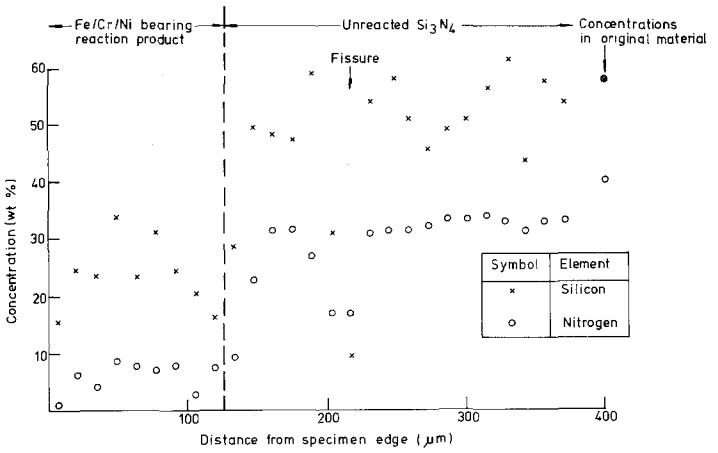

Figure 9 Silicon and nitrogen profiles across the reaction product formed in silicon nitride after 4644 h interaction with the Hastelloy X alloy at 1000° C.

alloy its distribution from the surface was consistent with a diffusion profile, whilst with the remaining alloys which contained a constituent, such as Ti, Al or Y, forming a stable nitride, nitrogen reacted with these constituents. On the PE 16 alloy reaction was restricted to the surface; with Fecralloy steel it occurred preferentially at the grain boundaries. while with the Nimonic 75 alloy titanium nitride was precipitated randomly throughout the alloy. The presence of these nitrides and also in the case of the PE 16 and Hastelloy X alloys of molybdenum silicide, increased the

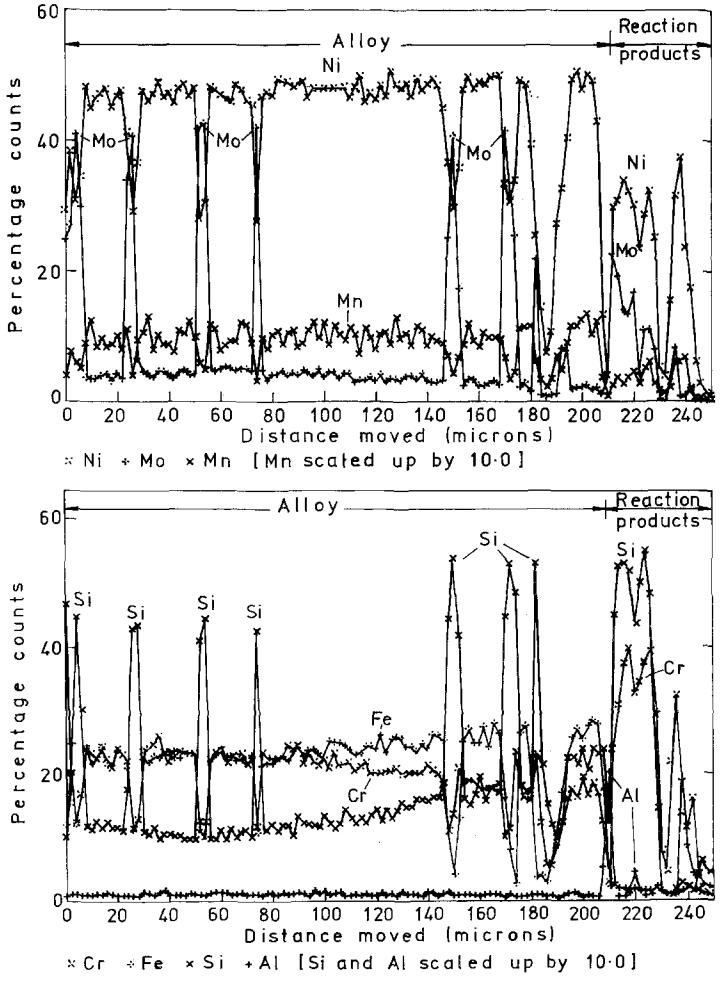

Figure 10 EPMA of the Hastelloy X alloy after 1173 h reaction with Si_3N_4 at 1000° C. (The elemental traces were for the same traverse across the alloy and reaction products.

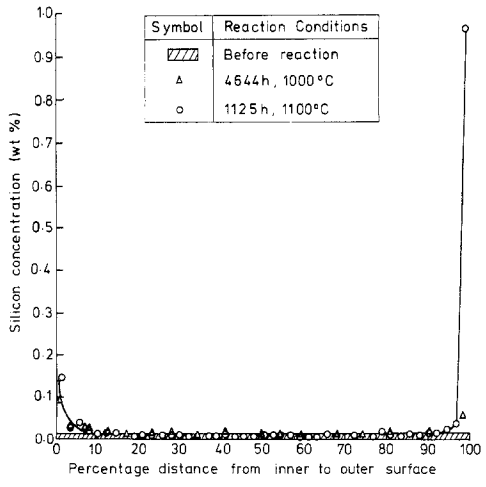

Figure 11 Silicon penetration into the TZM alloy from the interaction with silicon nitride at 1000 and 1100° C.

adhesion of the silicide–nitride reaction product to the alloy. In contrast, with the austenitic stainless steels, in which neither these nitrides nor the silicide were formed, the solid reaction products did not adhere to the alloys.

At 900° C silicon was taken up only by the 316 and 20/25/Nb steels reflecting their higher reactivity. At 1000° C silicon uptakes by all alloys were substantial. Well-defined diffusion profiles were observed from the surface into the alloys, except in the Hastelloy X alloy after a long exposure and in the Fecralloy steel, where the silicon was distributed randomly across the alloy. In the alloys containing molybdenum (i.e. the PE 16 and Hastelloy X alloys) silicon tended to be associated with this element.

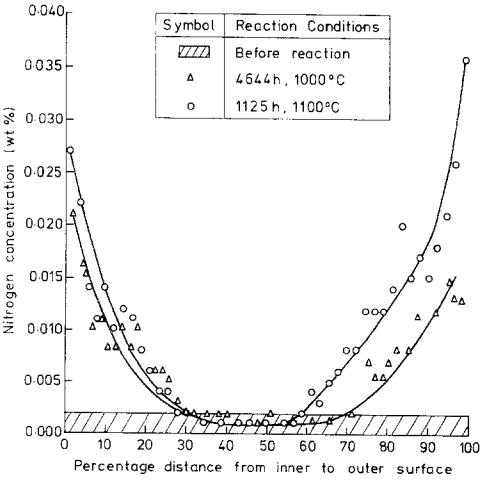

Figure 12 Nitrogen penetration into the TZM alloy from the interaction with the silicon nitride at 1000 and 1100° C.

The silicon and nitrogen uptakes by the TZM alloy could have resulted from a solid–solid reaction with dissolution of nitrogen into the alloy being the critical step. Alternatively thermal decomposition of silicon nitride may have freed the elements for subsequent reaction with the alloy.

5. Conclusions

(1) A primary reaction was involved in the solid–solid interaction at 800 to 1100° C in gettered inert gas between silicon nitride and the range of iron- and nickel-based alloys (AISI 316 and 20/25/Nb austenitic stainless steels, Fecralloy (with and without yttrium) ferritic stainless steels, nickel-based PE 16, Hastelloy X and Nimonic 75 alloys). It involved the reaction of chromium and also where appropriate iron and/or nickel with the nitride to form basically a silicide, which also contained nitrogen.

(2) The temperature for the onset of measurable reaction was between 825 and 900° C, depending on the alloy. Interaction with all alloys was appreciable at 1000° C, being greatest with the 20/25/Nb steel and least with the Fecralloy steel. It tended to increase with the chromium content of the alloy.

(3) Silicon and nitrogen were produced by the decomposition of the primary reaction product. Either or both of these elements were taken up by the alloys. Silicon diffused into the alloys and tended to be associated with molybdenum in the PE 16 and Hastelloy X alloys containing this element. There were several types of nitrogen pick-up. Only on the Hastelloy X alloy did the uptake follow a diffusion profile. Nitrogen reacted with some alloy constituents such as Ti, Al and Y forming a stable nitride. In contrast surface layers on the austenitic steels were denitrided, with the nitrogen being transferred to the tantalum getter.

(4) With the TZM alloy no alloy constituent was transferred to the silicon nitride. However, a silicon layer built up at the alloy surface, while nitrogen was picked up, with its penetration from the surface following a diffusion profile.

Acknowledgements

We gratefully acknowledge the experimental contribution to this study by J. Watling (X-ray fluorescence), J. W. McMillan and F. C. W. Pummery (nuclear microprobe analysis), Dr D. M.

Poole (EPMA), J. E. Bainbridge (EDAX analysis), J. B. Warburton and R. F. A. Carney. We also wish to thank Dr J. E. Antill for helpful discussions.

References

1. E. H. ANDREWS, *J. Mater. Sci.* **1** (1966) 377.
2. C. A. CALOW and R. B. BARCLAY *ibid.* **2** (1967) 404.
3. E. H. ANDREWS, W. BONFIELD, C. K. L. DAVIES and A. J. MARKHAM, *ibid.* **7** (1972) 1003.
4. R. L. MEHAN and D. W. McKEE, *ibid.* **11** (1976) 1009.
5. J. W. McMILLAN and F. C. W. PUMMERY, *J. Radioanl. Chem.* **38** (1977) 51.
6. H. D. BATHA and E. D. WHITNEY, *J.A.C.S.* **56** (1973) 365.

Received 5 May and accepted 20 June 1978.